ACS APPLIED MATERIALS & INTERFACES

Research Article

www.acsami.org

New Antifouling Platform Characterized by Single-Molecule Imaging

Ji Young Ryu,[‡,⊥] In Taek Song,[†,⊥] K. H. Aaron Lau,[§,∥] Phillip B. Messersmith,[§] Tae-Young Yoon,*[,‡] and Haeshin Lee*[,†]

[†]Department of Chemistry, [‡]National Creative Research Initiative Center for Single-Molecule Systems Biology, and Department of Physics, KAIST, 291 University Rd., Daejeon 305-701, Republic of Korea

[§]Biomedical Engineering Department, Northwestern University, Evanston, Illinois 60208, United States

Supporting Information

ABSTRACT: Antifouling surfaces have been widely studied for their importance in medical devices and industry. Antifouling surfaces mostly achieved by methoxy-poly(ethylene glycol) (mPEG) have shown biomolecular adsorption less than 1 ng/cm^2 which was measured by surface analytical tools such as surface plasmon resonance (SPR) spectroscopy, quartz crystal microbalance (QCM), or optical waveguide lightmode (OWL) spectroscopy. Herein, we utilize a single-molecule imaging technique (i.e., an ultimate resolution) to study antifouling properties of functionalized surfaces. We found that about 600 immunoglobulin G (IgG) molecules are adsorbed. This result corresponds to ~5 pg/cm^2 adsorption, which is far below amount for the detection limit of the conventional tools. Furthermore, we developed a new antifouling platform that exhibits improved antifouling performance that shows only 78 IgG molecules adsorbed (~0.5 pg/cm^2). The antifouling platform consists of forming 1 nm TiO_2 thin layer, on which peptidomimetic antifouling polymer (PMAP) is robustly anchored. The unprecedented antifouling performance can potentially revolutionize a variety of research fields such as single-molecule imaging, medical devices, biosensors, and others.

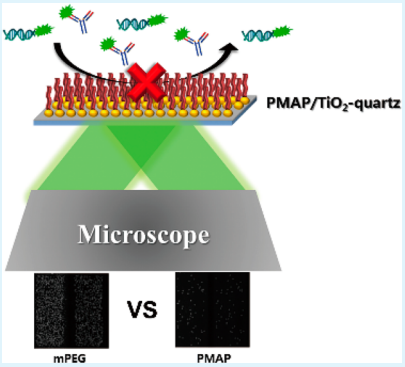

KEYWORDS: *antifouling, TiO_2 coating, catecholamine, polypeptoid, single-molecule imaging*

INTRODUCTION

The past decade has witnessed the use of surface-based single-molecule experiments to shed light on many important, but previously obscure, biological processes. Typically, individual molecules of interest are immobilized at a surface, permitting continuous observation of the same single molecules under different molecular conditions. Passivation of the surface onto which the single molecules are immobilized is the basic requirement for success of such surface-based single-molecule experiments. In the case of studying binding and unbinding kinetics of substrates, incomplete passivation of the surface causes nonspecific binding of substrate molecules, producing false positive results and precluding measurement of a true kinetic rate. Even when conformational changes within single molecules are observed, irregularities on the surface could induce behavior of the single molecules different from what occurs under physiological conditions, thereby producing results regarded as surface artifacts.

A recent advance in surface-based single-molecule experiments involves measurements with unpurified samples. These experiments, which directly image processes occurring in the cell or tissue extracts, enable the study of large protein complexes[1] and cell signaling proteins freshly derived from individual cancers,[2] which would be almost inaccessible with the conventional single-molecule measurements designed for synthetic nucleic acids and/or purified recombinant proteins. It is noteworthy that single-molecule experiments performed in a complex biological fluid require a more strict level of surface passivation. Typically, the ratio of a target protein to all other proteins in an unpurified lysate is only 10^{-3} even for the most abundant species. Nonspecific binding of these other proteins, larger in quantity by 3 orders of magnitude, on the surface can produce spurious interactions with substrates, making it impossible to separate the specific interaction of the target proteins. Thus, there is an obvious technical need to improve the antifouling performance of single-molecule imaging surfaces.

Methoxy-polyethylene glycol (mPEG) has been used as the standard material for preparing antifouling surface.[3,4] Because of hydration and brush like effect achieved at high surface density, an mPEG-coated surface shows resistance against nonspecific binding of biomacromolecules.[5,6] However, mPEG has several limitations. Long exposure (extended to few months) of mPEG to high temperature with oxidative radicals in aqueous environments results in hydrolysis.[6−8] Also, the current protocol for mPEG coating of oxides involves two reaction steps, amino-silane coating and mPEG-NHS reaction, which are difficult to control and can lead to low grafting efficiency of mPEG.

Received: December 13, 2013
Accepted: February 6, 2014
Published: February 6, 2014

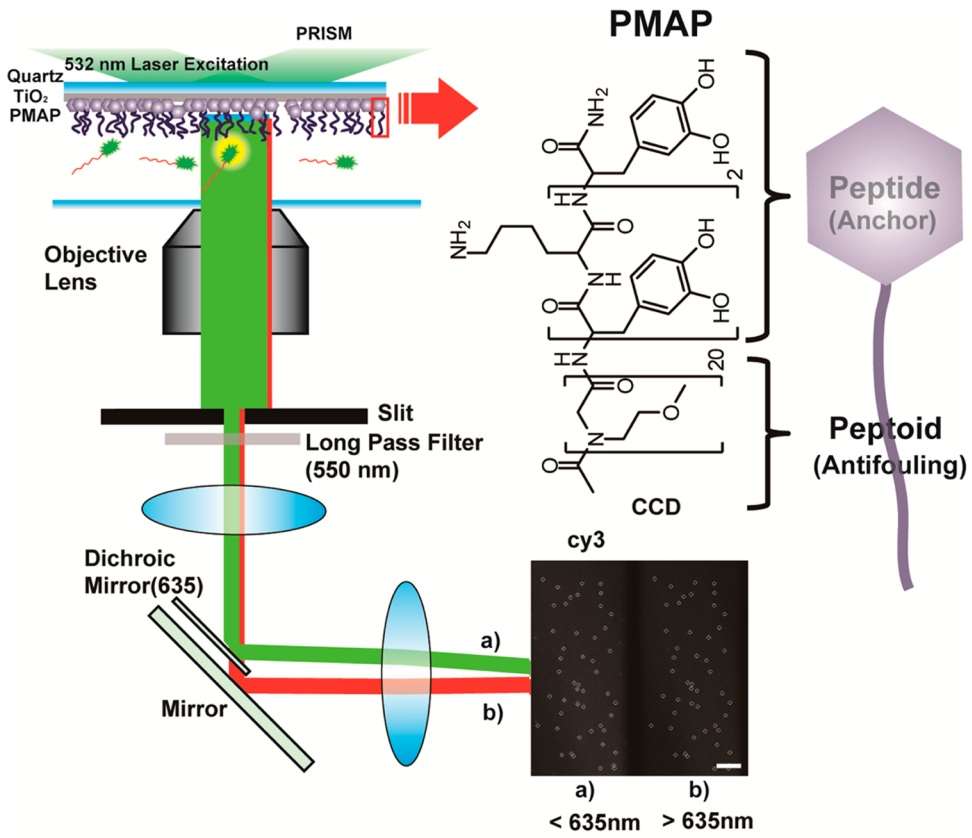

Figure 1. Experimental setup based on PMAP/TiO_2-quartz and the structure of PMAP. Scale bar, 10 μm.

In this study, we report a new class of antifouling platform that is specifically adapted to the surface-based single-molecule experiment. Imaging of single-molecule adsorption is performed by total internal reflection (TIR) microscopy in which fluorescent molecules located near to surfaces (<200 nm) or directly contacted to surfaces can be excited by evanescence wave induced by incident laser and its subsequent total reflection. The platform combines a 1 nm TiO_2 layer, which is electron-beam deposited on a quartz slide, with peptidomimetic antifouling polymer coating (PMAP) (Figure 1, left). Single-molecule imaging under TIR microscope showed 2- to 10-fold improved antifouling activities compared to the conventional mPEG-coated surface. Using conventional approaches to mPEG grafting, about 600 IgG molecules were observed compared to 78 molecules adsorbed onto the newly developed PMAP/TiO_2 surfaces, a level equivalent to 0.00048 ng/cm^2 adsorption. This value is far below the detection limit of current surface analytical tools such as surface plasmon resonance (SPR) and optical waveguide lightmode (OWL) spectroscopy, which detect typically ~1 ng/cm^2.[9,10] Furthermore, in the TIR system, one dot in images represents one molecule adsorbed on the surface. (In the current imaging system, the diffraction limit is about 222 nm. Thus, a molecule with a dimension smaller than 222 nm will be shown as one spot on screen.) Thus, our new surface functionalization platform combines the use of TIR imaging with an improved antifouling polymer grafting strategy to allow single-molecule experiments with better resolution than is available with existing methods.

RESULT AND DISCUSSION

PMAP is a peptide-peptoid hybrid diblock copolymer.[11] Peptoids are poly(N-substituted glycine)s with substantial backbone conformational flexibility.[12] The antifouling peptoid block with 1-amino-2-methoxyethane side chains was prepared by conventional solid-phase submonomer synthesis. The peptide block was a mussel-inspired, catecholamine adhesive moiety of 3,4-dihydroxy-L-phenylalanine and lysine (DOPA-K) (Figure 1, right). The catecholamine moiety shows robust surface adhesion, mimicking the underwater adhesion of marine mussels. It was previously reported that the antifouling property of PMAP prevented adhesion of fibroblast cells up to 6 months.[13−15] However, a direct comparison of PMAP with mPEG has not been made, and it has not been shown yet whether the antifouling property of PMAP can be applied for surface-based single-molecule experiments.

To evaluate the level of antifouling efficacy, we performed single-molecule adsorption experiments utilizing fluorescently labeled DNAs (Cy3-labeled 14 nucleotide single-stranded DNA, Cy3−14 nt ssDNA) and proteins (Cy3-labeled immunoglobulin G, IgG). Passivation of the surface was assessed by exposing the surface to a buffered solution of the biomolecule for a period of time, followed by rinsing with pure buffer and counting nonspecifically bound single molecules per imaging area (45 × 90 μm^2, in our case).

Preliminary experiments on bare quartz showed suboptimal passivation by PMAP (see the Supporting Information), which we attributed to weak interaction between catecholamine and SiO_2 yielding low surface density of PMAP. Since it was previously demonstrated that catecholamine shows strong and robust binding to TiO_2,[11,16−18] we prepared a TiO_2-coated

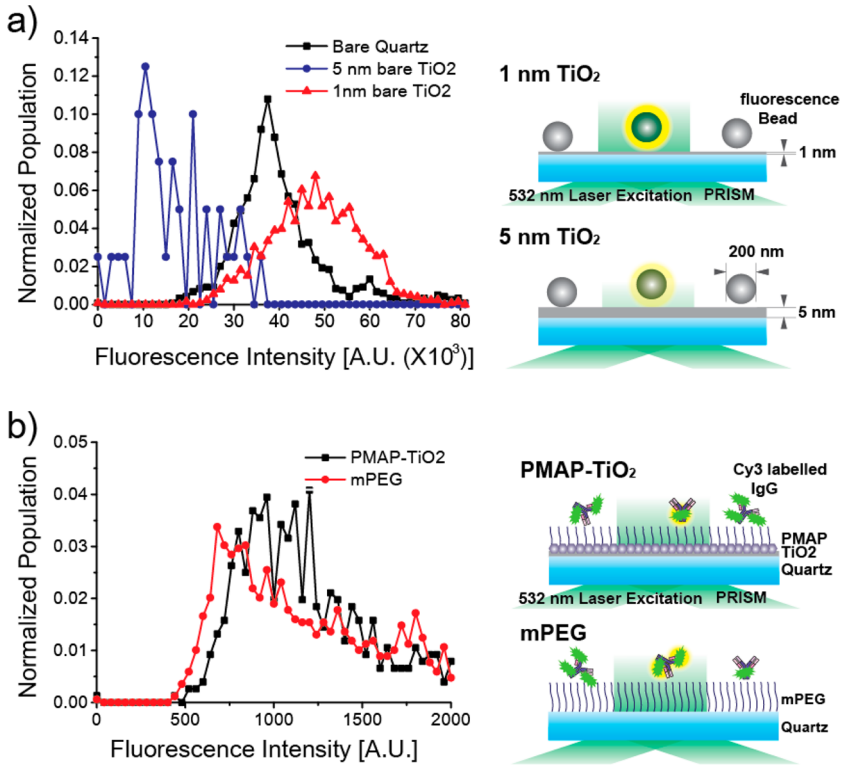

Figure 2. Optimization of TiO_2/quartz surface preparation for single-molecule imaging. (a) Distribution of fluorescent intensity from individual PS particle adsorbed on bare quartz (black, molecule n = 1194), 1 nm (red, molecule n = 1256), and 5 nm coating (blue, molecule n = 39) of TiO_2. (b) Fluorescent intensity distribution from individual Cy3-Oligo-DNA adsorbed on bare quartz (red, molecule n = 1688) and 1 nm Ti (black, molecule n = 759).

quartz substrate and formed PMAP layer on the TiO_2 surface. One complication of this design, however, is that TiO_2 would reduce the number of transmitted photons because of both its high real part of the refractive index (2–3) and formation of nanosize-metal grains.[19,20] When we measured the fluorescence signals of fluorescently labeled polystyrene beads (0.2 μm diameter) under TIR excitation, the 5 nm thick TiO_2 layer substantially reduced the fluorescence intensity of individual beads because of attenuation of excitation photons (λ = 532 nm) (Figure 2a, blue versus black symbols). On the contrary, when the TiO_2 layer was decreased to 1 nm, it was interesting to see the fluorescence intensity of beads recovered (Figure 2a, red symbols). In fact, the fluorescence intensity in the presence of 1 nm TiO_2 layer was slightly enhanced compared with the case with the bare quartz surface (Figure 2a, red versus black symbols), which was probably due to the effect of metal-induced fluorescence enhancement.[21]

We validated this observation of enhanced fluorescence at the single-molecule level. We measured the fluorescence intensity of residual nonspecifically bound Cy3-labeled IgG proteins on the PMAP/1 nm TiO_2/quartz surface. Their fluorescence intensity was slightly enhanced compared with that observed on the mPEG/quartz surface (Figure 2b). On the basis of these results, we chose the 1 nm thickness for the TiO_2 layer formed on the quartz surface.

Next, we studied different conditions for PMAP coating by varying the reaction time (12 and 24 h) and temperature (37 and 60 °C). We studied the nonfouling properties of these PMAP/TiO_2/quartz surfaces with the nonspecific binding test using 100 nM Cy3–14 nt ssDNA (5 min incubation). The nonspecific binding numbers were 308 ± 67.8 for 12 h incubation at 37 °C, 255 ± 33.6 for 24 h incubation at 37 °C, 55 ± 18.7 for the 12 h incubation at 60 °C and 12 ± 7.25 for the 24 h incubation at 60 °C (all errors are S.D.) (Figure 3). The results demonstrate that the PMAP layer coated on the 1 nm TiO_2/quartz surface, prepared through 24 h incubation at

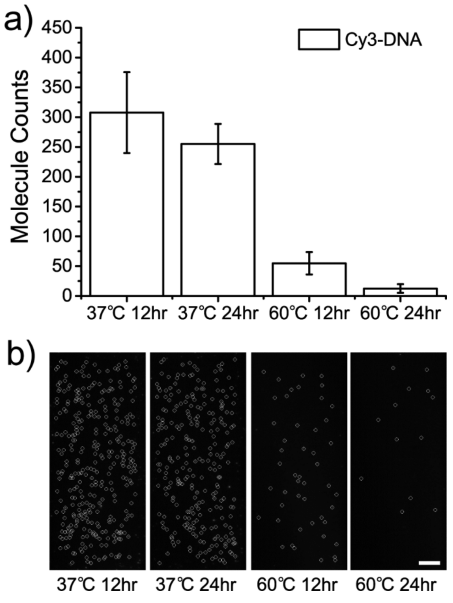

Figure 3. Optimization of PMAP coating conditions. (a) Counting adsorption Cy3-Oligo-DNA molecules per imaging area (45 × 90 μm^2) under various conditions. (b) Snapshots of Cy3-Oligo-DNA molecule images in each condition. Scale bar, 10 μm.

dx.doi.org/10.1021/am4057387 | ACS Appl. Mater. Interfaces 2014, 6, 3553–3558

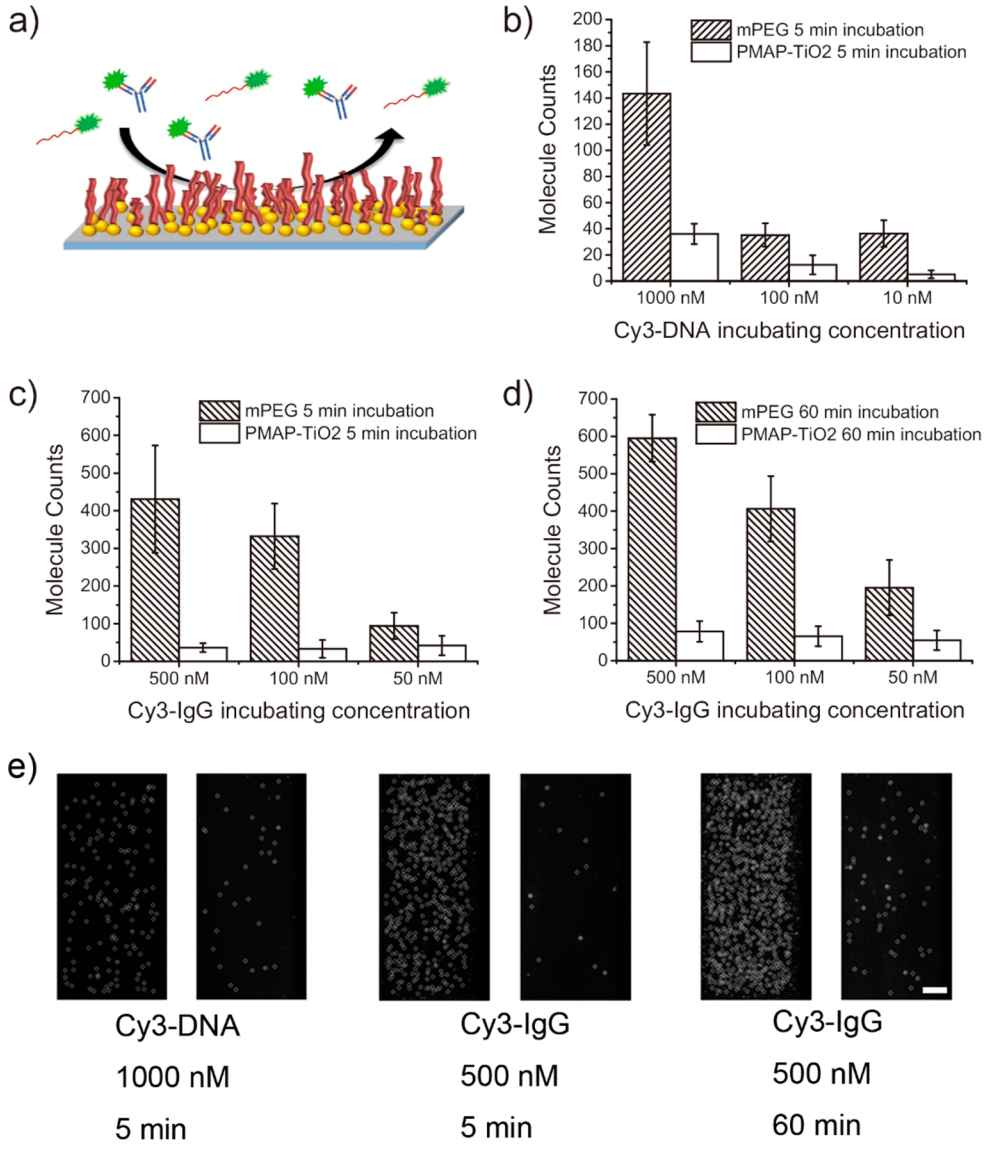

Figure 4. Antifouling effects of PMAP/TiO_2-quartz. (a) Schematic of antifouling effect of PMAP experiment for Cy3-Oligo-DNA, Cy3-IgG. (b) Results for PMAP-coated surfaces exposed to Cy3-Oligo-DNA for 5 min. The number of Cy3-Oligo-DNA adsorbed on mPEG surfaces (diagonal pattern) and PMAP surfaces (blank) are shown in the bar graph (n = 20). (c) Results for PMAP-coated surfaces exposed to Cy3-IgG for 5 min. The number of Cy3-IgG modified on mPEG surfaces (diagonal pattern) and PMAP surfaces (blank) are shown in the graph (n = 20). (d) Results for PMAP-coated surface exposed to Cy3-IgG for 60 min incubation. For 60 min, The numbers of Cy3-IgG absorbed on mPEG surfaces (diagonal pattern) and PMAP surfaces (blank) are displayed in the bar graph (n = 20). (e) Protein adsorption images for 1000 nM Cy3-DNA (1st, 2nd), 500 nM Cy3-IgG 5 min incubation (3rd, 4th), for IgG 60 min incubation (5th, 6th). Representative CCD images are shown in Supporting Information Figure S3. Scale bar, 10 μm.

60 °C, showed the best antifouling property. In a similar fashion, the PEG immobilization condition was investigated to identify grafting conditions yielding optimal nonfouling property. We chose a cloud point condition (0.6 M K_2SO_4, 0.1 M MOPS, pH 6.0), which was demonstrated to increase surface density of the immobilized PEG brush.[22] We observed about 20−40% improvement in nonfouling property at high concentrations (>100 nM of IgG). However, this improvement was not significant for single-molecule experiments. Our experimental aim was to achieve less than 100 adsorbed molecules at high concentrations (>100 nM) of proteins and DNA. Under cloud point adsorption conditions results showed that 177 molecules were adsorbed for 100 nM and 325 molecules were found for 500 nM (Figure S2). Since PEG is widely used by single-molecule researchers, we therefore decided to compare the mPEG and PMAP coated surfaces in our subsequent experiments.

The antifouling property of the PMAP/TiO_2/quartz surface was first assessed using Cy3−14 nt ssDNAs by varying the DNA concentration from 10 to 1000 nM. The nonspecific binding onto PMAP/TiO_2/quartz surface was significantly reduced compared to mPEG/quartz, showing less than a hundred molecules adsorbed at all DNA concentrations studied.

At 10 nM, 5 ± 3.07 DNA molecules were adsorbed on the PMAP/TiO_2/quartz surface while 36 ± 10.2 molecules were detected on the mPEG/quartz surface (Figure 4b). The difference became even larger at 1 μM; only 36 ± 7.8 spots were detected for the PMAP/TiO_2/quartz surface, which was much smaller than 143 ± 39.4 observed for mPEG/quartz

dx.doi.org/10.1021/am4057387 | ACS Appl. Mater. Interfaces 2014, 6, 3553−3558

surface (Figure 4b). Considering that 1 μM is a typical DNA concentration observed in a cell or tissue extract,[23] our results suggest that the PMAP/PMAP/TiO_2/quartz surface has an antifouling property sufficient to suppress nonspecific adsorption of nucleic acid molecules present in a dense lysate condition.

We studied nonspecific adsorption of Cy3-labeled IgG as a prototypic protein.[24] After 5 min incubation, the enhanced nonfouling effect of the PMAP/TiO_2/quartz surface was apparent. At 500 nM, the PMAP/TiO_2/quartz surface showed adsorption of only 37 ± 11.9 IgG proteins, but the mPEG/quartz surface showed 431 ± 142.5 proteins per imaging area (Figure 4c), showing 1 order of magnitude difference in protein adsorption. Under more dilute conditions a similar trend was observed: 33 ± 23.8 (PMAP) versus 331 ± 87.0 (mPEG) at 100 nM and 42 ± 25.8 (PMAP) versus 94 ± 35.1 (mPEG) for 10 nM (n = 20).

The advantage afforded by PMAP over mPEG was reaffirmed when the surface was exposed to IgG proteins for 1 h. The PMAP/TiO_2/quartz surface showed nonspecific binding of only 78 ± 27.5 at 500 nM, 66 ± 27.1 at 100 nM, and 55 ± 26.3 at 50 nM, whereas 595 ± 62.7 at 500 nM, 406 ± 87.1 at 100 nM, and 195 ± 74.2 at 50 nM was observed for the mPEG/quartz surface (Figure 4d). Figure 4e shows the representative CCD images of DNA or protein surface adsorption for the highest concentrations of each biomacromolecule: 1000 nM DNA (1st and 2nd; equivalent to the graph shown in panel b), 500 nM IgG for 5 min incubation (3rd and 4th; the data shown in panel c), and 500 nM IgG for 60 min incubation (5th and 6th; the data shown in panel d).

Our results demonstrate that the PMAP/TiO_2/quartz surface is robust against protein adsorption even when the protein concentration is at hundreds of nM. Given that the concentration threshold for single-molecule imaging is ∼100 nM under conventional TIR excitation, our PMAP/TiO_2/quartz surface is expected to provide a higher signal-to-noise ratio and allow the detection of weak protein−protein interactions by reducing the nonspecific binding of biomacromolecules to substrates. Furthermore, PMAP is resistant against enzymatic hydrolysis due to its non-natural polypeptoide backbone,[25−27] a desirable property when imaging processes in a whole lysate where the presence of protease proteins are unavoidable.

CONCLUSION

In conclusion, we have established a new antifouling system that consists of a thin (1 nm) coating of TiO_2 on quartz, followed by immobilization of mussel-inspired catecholamine-polypeptoid (PMAP). For all the cases examined, the newly developed PMAP/TiO_2/quartz surface exhibits a vastly improved antifouling property compared with the conventional mPEG/quartz surface. We expect that the PMAP/TiO_2/quartz surface will provide a surface inert enough to allow the surface-based single-molecule experiments to tackle more heterogeneous, but biologically more important systems.

ASSOCIATED CONTENT

Supporting Information

Experimental protocol and additional supporting details and figures. This material is available free of charge via the Internet at http://pubs.acs.org.

AUTHOR INFORMATION

Corresponding Authors

*E-mail: tyyoon@kaist.ac.kr.
*E-mail: Haeshin@kaist.ac.kr.

Present Address

[‖]K.H.A.L.: Department of Pure and Applied Chemistry, University of Strathclyde, Glasgow, U.K.

Author Contributions

[⊥]J.Y.R. and I.T.S.contributed equally. The manuscript was written through contributions of all authors. All authors have given approval to the final version of the manuscript.

Notes

The authors declare no competing financial interest.

ACKNOWLEDGMENTS

The authors are thankful to Dr. Hyun Ok Ham for PMAP synthesis. This work was supported by National Research Foundation of Republic of Korea: National Creative Research Initiative (Center for Single-Molecule Systems Biology to T.-Y.Y. N01130069), Molecular-level Interface Research Center (20090083525, H.L.), and Biomedical Technology Development Program (2009-0092222, H.L.). Partial support was also provided by National Institutes of Health Grants 2R01EB005772-05A1 and National Heart, Blood and Lung Institute (NHBLI) (HL104966) at the NIH. This study is also supported by POSCO Chung-Am Foundation (H.L.).

REFERENCES

(1) Hoskins, A. A.; Friedman, L. J.; Gallagher, S. S.; Crawford, D. J.; Anderson, E. G.; Wombacher, R.; Ramirez, N.; Cornish, V. W.; Gelles, J.; Moore, M. J. Ordered and Dynamic Assembly of Single Spliceosomes. *Science* **2011**, *331*, 1289−1295.

(2) Lee, H. W.; Kyung, T.; Yoo, J.; Kim, T.; Chung, C.; Ryu, J. R.; Lee, H.; Park, K.; Lee, S.; Jones, W. D.; Lim, D. S.; Hyeon, C.; Heo, W. D.; Yoon, T. Y. Real-time Single-molecule Co-immunoprecipitation Analyses Reveal Cancer-specific Ras Signalling Dynamics. *Nat. Commun.* **2013**, *4*, 1505.

(3) Harris, J. M.; Zalipsky, S. *Poly(ethylene glycol): Chemistry and Biological Applications*; American Chemical Society: Washington, DC, 1997.

(4) Zhang, F.; Kang, E. T.; Neoh, K. G.; Huang, W. J. Modification of Gold Surface by Grafting of Poly(ethylene glycol) for Reduction in Protein Adsorption and Platelet Adhesion. *J. Biomater. Sci., Polym. Ed.* **2001**, *12*, 515−531.

(5) Dalsin, J. L.; Messersmith, P. B. Bioinspired Antifouling Polymers. *Mater. Today* **2005**, *8*, 38.

(6) Ostuni, E.; Chapman, R. G.; Holmlin, R. E.; Takayama, S.; Whitesides, G. M. A Survey of Structure-property Relationships of Surfaces that Resist the Adsorption of Protein. *Langmuir* **2001**, *17*, 5605−5620.

(7) Han, S.; Kim, C.; Kwon, D. Thermal/oxidative Degradation and Stabilization of Polyethylene glycol. *Polymer* **1997**, *38*, 317−323.

(8) Jiang, S.; Cao, Z. Ultralow-Fouling, Functionalizable, and Hydrolyzable Zwitterionic Materials and Their Derivatives for Biological Applications. *Adv. Mater.* **2010**, *22* (9), 920−932.

(9) Konradi, R.; Acikgoz, C.; Textor, M. Polyoxazolines for Nonfouling Surface Coatings −A Direct Comparison to the Gold Standard PEG. *Macromol. Rapid Commun.* **2012**, *33*, 1663−1676.

(10) Blaszykowski, C.; Sheikh, S.; Thompson, M. Surface Chemistry to Minimize Fouling from Blood-based Fluids. *Chem. Soc. Rev.* **2012**, *41*, 5599−5612.

(11) Statz, A. R.; Meagher, R. J.; Barron, A. E.; Messersmith, P. B. New Peptidomimetic Polymers for Antifouling Surfaces. *J. Am. Chem. Soc.* **2005**, *127*, 7972−7973.

(12) Rosales, A. M.; Segalman, R A.; Zuckermann, R. N. Polypeptoids: A Model System to Study the Effect of Monomer Sequence on Polymer Properties and Self-assembly. *Soft Matter* **2013**, *9*, 8400−8414.
(13) Lee, H.; Dellatore, S. M.; Miller, W. M.; Messersmith, P. B. Mussel-inspired Surface Chemistry for Multifunctional Coatings. *Science* **2007**, *318*, 426−430.
(14) Waite, J. H.; Tanzer, M. L. Polyphenolic Substance of Mytilus Edulis − Novel Adhesive Containing L-Dopa and Hydroxyproline. *Science* **1981**, *212*, 1038−1040.
(15) Waite, J. H.; Qin, X. X. Polyphosphoprotein form the Adhesive Pads of Mytilus Edulis. *Biochemistry* **2001**, *40*, 2887−2893.
(16) Creutz, C.; Chou, M. H. Binding of Catechols to Mononuclear Titanium (IV) and to 1- and 5-nm TiO_2 nanoparticles. *Inorg. Chem.* **2008**, *47*, 3509−3514.
(17) Rodenstein, M.; Zurcher, S.; Tosatti, S. G. P.; Spencer, N. D. Fabricating Chemical Gradients on Oxide Surfaces by Means of Fluorinated, Catechol-Based, Self-Assembled Monolayers. *Langmuir* **2010**, *26*, 16211−16220.
(18) Lee, H.; Scherer, N. F.; Messersmith, P. B. Single-molecule Mechanics of Mussel Adhesion. *Proc. Natl. Acad. Sci. U.S.A.* **2006**, *103*, 12999−13003.
(19) Bennett, J. M.; Pelletier, E.; Albrand, G.; Borgogno, J. P.; Lazarides, B.; Carniglia, C. K.; Schmell, R. A.; Allen, T. H.; Tuttle-Hart, T.; Guenther, K. H.; Saxer, A. Comparison of the Properties of Titanium Dioxide Films Prepared by Various Techniques. *Appl. Opt.* **1989**, *28*, 3303−3317.
(20) Tian, G. L.; He, H. B.; Shao, J. D. Effect of Microstructure of TiO_2 Thin Films on Optical Band Gap Energy. *Chin. Phys. Lett.* **2005**, *22*, 1787−1789.
(21) Ulatowska-Jarza, A.; Pucinska, J.; Wysocka-Krol, K.; Holowacz, I.; Podbielska, H. B. Nanotechnology for Biomedical Applications − Enhancement of Photodynamic Activity by Nanomaterials. *Bull. Pol. Acad. Sci.: Tech. Sci.* **2011**, *59*, 253−261.
(22) Kingshott, P.; Thissen, H.; Griesser, H. J. Effect of Cloud-point Grafting, Chain Length, and Density of PEG Layers on Competitive Adsorption of ocular Proteins. *Biomaterials* **2002**, *23*, 2043−2056.
(23) Downs, T. R.; Wilfinger, W. W. Fluorometric Quantification of DNA in Cells and Tissue. *Anal. Biochem.* **1983**, *131*, 538−547.
(24) Gonzalez-Quintela, A.; Alende, R.; Gude, F.; Campos, J.; Rey, J.; Meijide, L. M.; Fernandez-Merino, C.; Vidal, C. Clinical. Serum Levels of Immunogloblins (IgG, IgA, IgM) in a General Adult Population and Their Relationship with Alcohol Consumption, Smoking and Common Metabolic Abnormalities. *Clin. Exp. Immunol.* **2008**, *151*, 42−50.
(25) Miller, S. M.; Simon, R. J.; Ng, S.; Zuckermann, R. N.; Kerr, J. M.; Moos, W. H. Comparison of the Proteolytic Susceptibilities of Homologous L-Amino-Acid, D-Amino-Acid, and N-Substituted Glycine Peptide and Peptoid Oligomers. *Drug Dev. Res.* **1995**, *35*, 20−32.
(26) Simon, R. J.; Kania, R. S.; Zuckermann, R. N.; Huebner, V. D.; Jewell, D. A.; Banville, S.; Ng, S.; Wang, L.; Rosenberg, S.; Mar-lowe, C. K.; Spellmeyer, D. C.; Tan, R. Y.; Frankel, A. D.; Santi, D. V.; Cohen, F. E.; Bartlett, P. A. Peptoids − a Modular Approach to Drug Discovery. *Proc. Natl. Acad. Sci. U.S.A.* **1992**, *89*, 9367−9371.
(27) Zuckermann, R. N.; Kerr, J. M.; Kent, S. B. H.; Moos, W. H. Efficient Method for the Preparation of Peptoids [Oligo(N-Substituted Glycines)] by Submonomer Solid-Phase Synthesis. *J. Am. Chem. Soc.* **1992**, *114*, 10646−10647.